

GCSS VII: DYCOMS RF01

Bjorn Stevens and Chin-Hoh Moeng

June 6, 2003

Contents

1. Motivation	2
2. Case Specification	4
a. Mean State	4
b. Radiative forcing	5
3. Numerical Issues	7
4. Plan of Attack	8
5. Desired Output	8
6. Wait, Stop, Check!	11

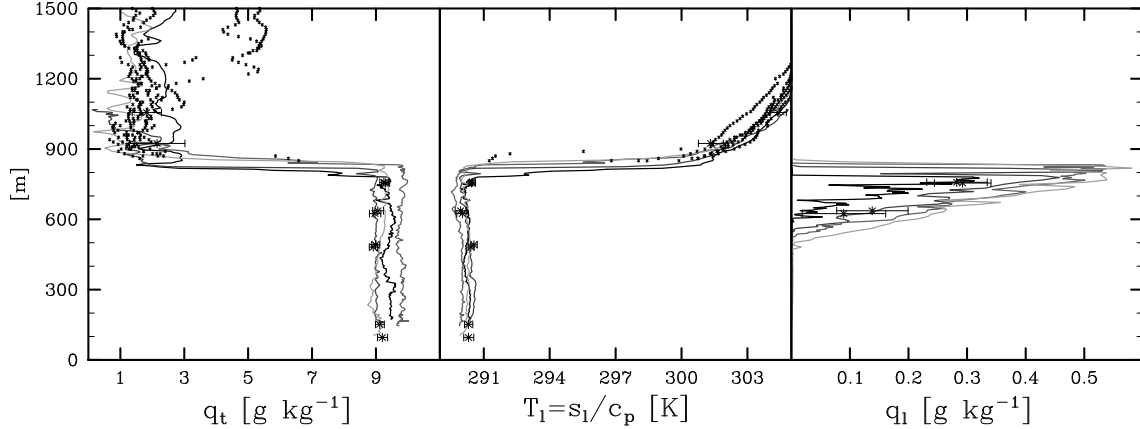


Figure 1: Cloud sounding data adapted from (Stevens et al., 2003)

1. Motivation

Our purpose is to evaluate Large-Eddy Simulation of Stratocumulus using a case-study approach. The case-study is chosen from the first flight of DYCOMS-II and is an elaboration of simulations performed in support of initial analyses of this flight (Stevens et al., 2003), which provides essential background for this case. The basic questions which this and previous analyses have posed, and which we will attempt to answer in this study, are the following:

1. Can LES produce the observed cloud evolution?
2. Can LES maintain the observed mixing line structure at cloud top?
3. Does the satisfaction of the Randall-Deardorff criterion for CTEI imprint itself on the cloud evolution in any noticeable way?
4. To what extent is boundary projection a proper way to cast the forcing?
5. To what extent do detailed radiative processes in the clear air above cloud top (cf., Siems et al., 1993) determine the subsequent cloud evolution?
6. Can LES capture the higher order turbulent statistics (specifically third order velocity statistics and cloud top interfacial statistics) at the cloud top interface?

These questions are elaborated on in turn below.

The stratocumulus deck observed during RF01 of DYCOMS-II provides an interesting case study because its evolution was one of gradual deepening through the course of the flight, within a large-scale environment which was remarkably constant in time. The basic structure of the cloud deck is illustrated with sounding data in Fig. 1. The variability in cloud thickness apparent in the sounding is due mostly to the fact that the aircraft sampled the deck in a quasi-Lagrangian sense, where cloud base appeared to be lower to the north. Correcting for these biases leads to an estimate of cloud evolution during the course of the flight which is illustrated in the left panel of Fig. 2. Note that there is no apparent cloud thinning, and although the correlation of the best fit line for the evolution of cloud base is rather low, this is due to compensation

between moistening and warming tendencies within the layer (cf. Stevens et al. (2003)). Mixing line analysis of all the cloud penetrations does however indicate that the cloud-top interface was on the unstable side of the Randall-Deardorff CTEI criterion (right panel, Fig. 2). Hence our first three motivating questions above.

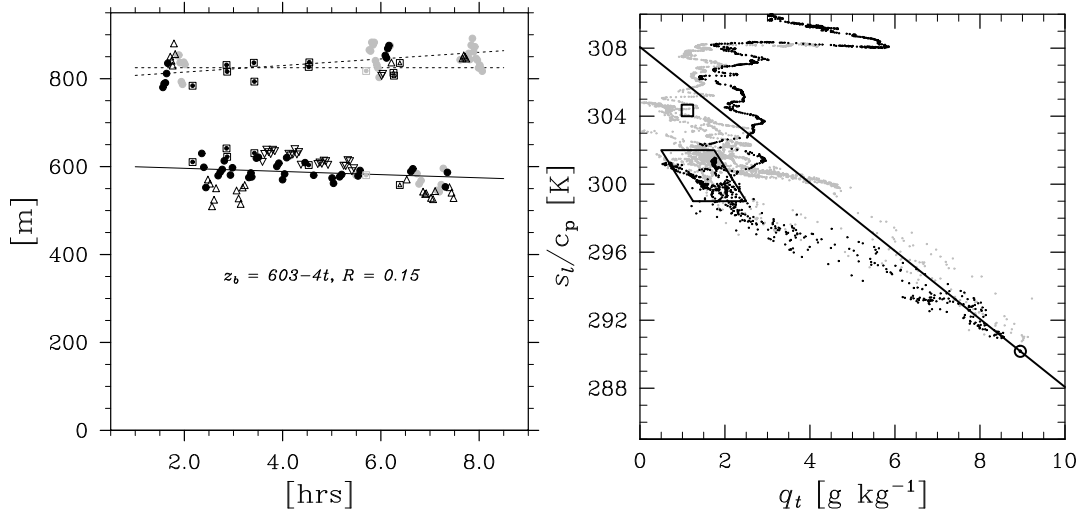


Figure 2: Temporal variation of cloud boundaries (left panel). Note the cloud base estimates for the central observational region are denoted by filled circles. These are the observations to which a linear trend was fitted, and to which we will compare the LES. Observations from this region are also denoted by blackened dots in mixing line plot (right panel) which shows data taken from cloud penetrations in central study region. Both figures are taken from (Stevens et al., 2003).

The fourth motivating question, called boundary projection, has to do with how to count the forcings in estimating the work done on cloud layers by diabatic processes, namely radiative fluxes (but also drizzle), which in actuality act throughout the cloud and boundary layer. For instance, in (Stevens, 2002) and in (Stevens et al., 2003) the radiative driving of the boundary layer is taken as the net radiative flux divergence acting across the boundary layer as a whole. This driving is then modeled as if it were only acting on a boundary. While this might seem reasonable for the cloud top radiative cooling, is it correct to count the cloud base warming in this fashion? During RF01, the former was approximately $70\ W\ m^{-2}$ while the latter was roughly $20\ W\ m^{-2}$, thus how one counts the latter's energetic contribution can be crucial. This issue also comes to the fore when we consider strategies for modeling the effect of drizzle on stratocumulus energetics. By having separate models of the cloud base warming and cloud top cooling radiative tendencies, a case study of RF01 seems like an excellent way to address this question. Because of its explicit representation of the large-eddies, LES is an ideal tool in this respect.

The fifth question arises from the observation that s_l above the cloud layer increases roughly as $(z - z_i)^{1/3}$. This implies a change in θ_l of $2K$ (equivalent to a 20% increase in the inversion strength over a distance of only 8m. To formulate jump conditions from the perspective of a mixed layer model, one needs to know the depth of the interfacial layer, and hence the effective stratification felt by the turbulent eddies as they push upward on the inversion. Thus it becomes interesting to investigate how enhanced cooling just above the cloud layer (which is thought to be responsible for the curvature in the θ_l there) interacts with dynamical processes, and helps determine the effective stability of the entrainment interface. To address this question we will specify a radiative flux profile which depends on the distance from cloud top in a way which produces the correct profile of θ_l in the limit of constant divergence with height.

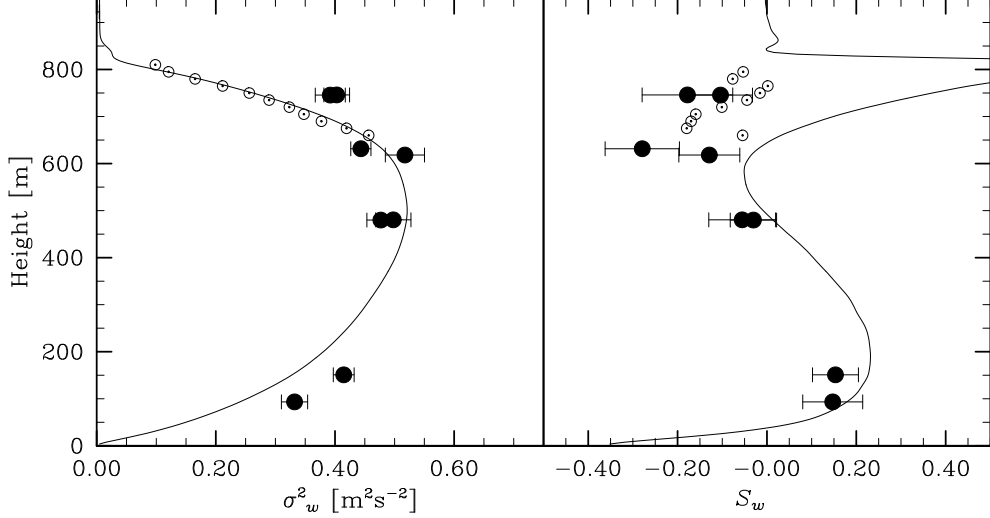


Figure 3: Vertical velocity variance and skewness, from simulation of RF01 (lines), radar retrieved Doppler velocity in weak echo sections of the cloud (circle-dot), and from *in situ* measurements (filled circle with uncertainty bar). Adapted from (Stevens et al., 2003)

The sixth question is motivated by Fig. 3 which shows the vertical velocity statistics from an exploratory simulation (e.g., Stevens et al., 2003) and those observed using *in situ* measurements and cloud radar. The main point of this figure is that despite reasonable agreement in the cloud variance statistics there is a marked departure between the simulation and the data in the vertical velocity skewness in the upper part of the cloud layer. This result is a more forceful statement of previous findings (Moeng and Rotunno, 1990; Moyer and Young, 1991, e.g.), which suggests that LES does not represent the higher order turbulent statistics in the vicinity of the cloud top interface with great fidelity.

2. Case Specification

a. Mean State

In specifying the mean state we desire to maintain several important features of the observed case through the spin up period of the simulation. These include the depth and continuity of the cloud layer, and the mixing line structure and inversion characteristics at cloud top. These basic characteristics are quantified in Table 1.

Quantity	Value
$\Delta\Theta_l$	10 K
Δr_t	7.5 g kg^{-1}
z_i	840 m
z_b	600 m
$q_l(z_{i-})$	0.475 g kg^{-1}

Table 1: Basic quantities whose values should be preserved through spin up period.

To generate a state which maintains these values we suggest starting with the following profiles of thermodynamic state variables:

$$\theta_l = \begin{cases} 289.0 \text{ K} & z \leq z_i, \\ 299.0 + (z - z_i)^{1/3} \text{ K} & z > z_i \end{cases} \quad (1)$$

$$q_t = \begin{cases} 9.0 \text{ g kg}^{-1} & z \leq z_i, \\ 1.5 \text{ g kg}^{-1} & z > z_i \end{cases} \quad (2)$$

In the above θ_l was defined from the surface air temperature using values of the physical constants given in Table 2, and a surface pressure of 1017.8 hPa. Note that c_p can vary substantially across the cloud top interface: for dry air $c_{pd} = 1005 \text{ J kg}^{-1} \text{ K}^{-1}$, while for water vapor $c_{pv} = 1870 \text{ J kg}^{-1} \text{ K}^{-1}$ which implies that the isobaric specific heat above the inversion is approximately $1008 \text{ J kg}^{-1} \text{ K}^{-1}$ and $1022 \text{ J kg}^{-1} \text{ K}^{-1}$ below. Hence our use of an intermediate value which excludes a dependence on the amount of ambient water vapor.

Quantity	Value
c_p	$1.015 \text{ kJ kg}^{-1} \text{ K}^{-1}$
R_d	$0.287 \text{ kJ kg}^{-1} \text{ K}^{-1}$
L_v	2.47 MJ kg^{-1}

Table 2: Suggested values of physical constants

To complete the specification of the basic case (absent the radiative forcing which is discussed in the following subsection) requires a determination of geostrophic winds, divergence, sea surface temperatures, and some indication of density for use in Boussinesq models. For the winds, we specify geostrophic values of $U_g = 7 \text{ m s}^{-1}$ and $V_g = -5.5 \text{ m s}^{-1}$ which produces winds within the boundary layer near 6 and 4.25 m s^{-1} respectively, as observed. One could choose to align the domain with the mean wind, however we do not do this to facilitate future investigations which may choose to examine the nature of momentum mixing within the stratocumulus topped boundary layer, and its affect on processes such as entrainment. The large-scale divergence of the winds is taken to be $D = 3.75 \times 10^{-6} \text{ s}^{-1}$ as this seems most consistent with the observed temperature structure above the boundary layer, and the calculated radiative forcing (see below). For the sea-surface temperature we specify a value of 292.5 K , which is 2.1 K warmer than the surface air temperature and should correspond to surface sensible heat fluxes near 20 W m^{-2} and surface latent heat fluxes of approximately 115 W m^{-2} given a bulk aerodynamic drag coefficient, $C_d = 0.0011$. The surface temperature and pressure correspond to a surface air density, $\rho_0 = 1.22 \text{ g kg}^{-1}$ and an air density just below cloud top of $\rho_i = 1.13 \text{ g kg}^{-1}$.

b. Radiative forcing

To parameterize the radiative forcing we use detailed calculations using the δ -four stream radiative transfer code developed by Fu and Liou 1993.. The radiative fluxes from this model are computed assuming the above specified state, matched to a free atmospheric sounding as discussed by Stevens et al. (2003). Note that to match the observed radiative fluxes a moist layer was incorporated into the radiative sounding at approximately 1500m . The results from this exercise are shown in Fig. 4.

Because a radiative calculation similar to the one used to make Fig. 4 is prohibitively expensive to incorporate into every column of a large-eddy simulation, we investigate the extent to which a simpler

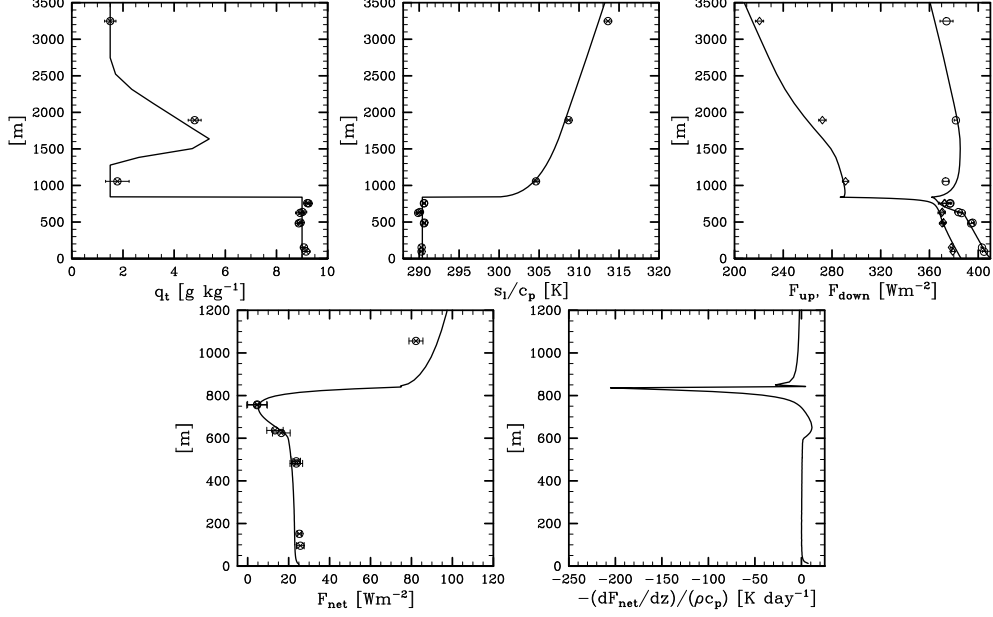


Figure 4: Plot of idealized soundings used to drive radiative calculations, and resulting radiative fields: q_t (upper left); s_l (upper center), F_{lw}^\downarrow and F_{lw}^\uparrow from calculations (lines) and measured (diamonds and circles respectively) upper right; net flux (lower left); heating rate (lower right). Note the different vertical scale on the lower plots. Adapted from (Stevens et al., 2003)

parameterization of radiative fluxes can be calibrated to represent the expected variations among columns for this case. In designing this scheme we sought to represent the main features of Fig. 4. Namely the significant flux divergence at cloud top, cloud base and just above cloud top, we also chose to use as a basis the simple form of the fluxes exploit in previous inter-comparison studies, (e.g., Bretherton et al., 1999). To do this we propose a three component model of the net radiative flux:

$$F(z) = F_0 \exp(-Q(z, \infty)) + F_1 \exp(-Q(0, z)) + \rho_i c_p D \left[\frac{(z - z_i)^{4/3}}{4} + z_i (z - z_i)^{1/3} \right], \quad (3)$$

where

$$Q(a, b) = \kappa \int_a^b \rho r_l dz, \quad (4)$$

and κ , F_0 and F_1 are tuning parameters. Note that the third term in (3) was chosen so that it generates the observed $(z - z_i)^{1/3}$ structure in the θ_l profile for $z > z_i$ and a large-scale subsidence velocity which varies linearly in z such that $W = -Dz$.

We find that this model gives a good fit to the δ -four stream approximation for the fluxes if we choose the parameter values specified in Table 3. This is illustrated in Fig. 5 where we show the fit for two cases, one being the control case with the specified cloud layer, the other being with a substantially drier boundary layer ($q_t = 8.5 \text{ g kg}^{-1}$) and hence a much thinner cloud ($q_{l,max} = 0.25 \text{ g kg}^{-1}$). These parameter values were adjusted by eye, so although the fit may not be optimal, it appears to be sufficient. Not only does (3) well represent the radiative fluxes as simulated by the δ -four stream model, it also appears to capture the basic nature of the sensitivity of these fluxes to significant changes in the state of the cloud layer.

Quantity	Value
F_0	70 W m^{-2}
F_1	22 W m^{-2}
κ	$85 \text{ m}^2 \text{ g}^{-1}$
D	3.75 s^{-1}

Table 3: Suggested parameter values for Eq. 3

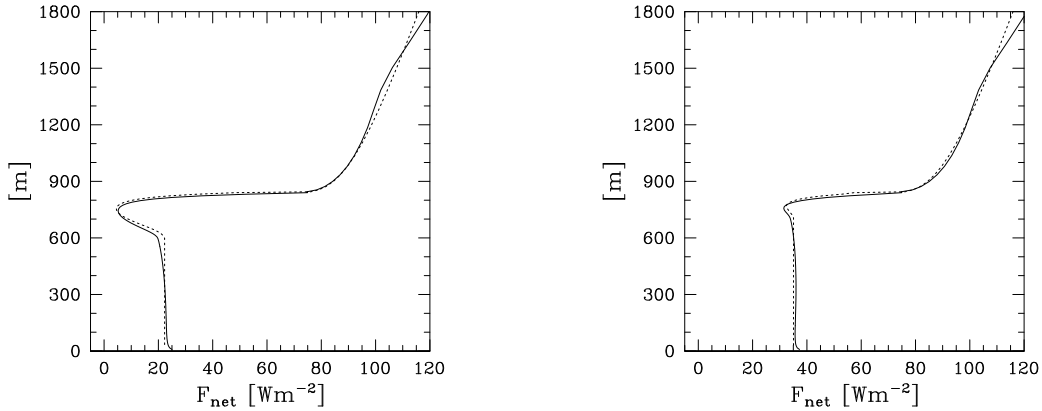


Figure 5: Plot of idealized net long-wave radiative flux from the δ -four stream and from Eq. 3 for the base case (left panel) and a drier boundary layer with a thinner cloud (right panel).

Note that this parameterization of the radiative fluxes raises a number of subsidiary questions. For instance, is such a parameterization appropriate for an undulating cloud top? Also, if the radiative flux divergences are so significant just above the cloud top, would they be sensitive to multi-dimensional effects within cloud crevices at the base of down-drafts? These are some additional questions which we may be able to address if we can perform reasonable simulations of the base case.

3. Numerical Issues

We are asking for this case to be integrated for four simulated hours, on a domain whose vertical extent is greater than 1250m. Note that the lapse rate of the specified temperature profile would equal the observed free atmospheric lapse rate of approximately 3.5 K km^{-1} at 1770 m, thus extending the domain beyond 1770 m would lead to increasingly large departures in the mean state unless the temperature profile is set to a constant lapse rate above 1770 m, and the radiative flux profiles are adjusted accordingly. Note, however that such departures from the observations are likely only to affect gravity wave propagation characteristics whose net effect on the simulation of the lower boundary layer are thought to be negligible.

The base case horizontal extent of the domain is to be 3.36 km with a nominal grid spacing of 35m, corresponding to 96 points in each horizontal direction. Because of the fine-scale thermal and radiative effects just above cloud top we are asking for simulations whose vertical discretization is 5m or less in the vicinity of the inversion.

Boussinesq models should use a base state density of 1.13 g m^{-3} , and anelastic models should be careful

to check that our failure to consider density variations with height in the formulation of Eq. 3 may alter the structure of the free-tropospheric temperature profile.

4. Plan of Attack

Preliminary tests of this case, by a number of participating groups, indicate that it is a challenging case to represent. For this reason we are asking participants to perform simulations with increasing complexity as enumerated below:

1. Simple forcing: A case with only longwave radiative cooling from cloud top active (at a value equal to the net forcing of the PBL, i.e., 48 Wm^{-2} see below, fixed thermodynamic fluxes (15 and 115 Wm^{-2} respectively) at the surface, and **no large-scale subsidence**.
2. Partial forcing: As above but with introduction of cloud base warming term.
3. Inversion forcing: Introduce subsidence and inversion layer cooling term.
4. Full forcing: Introduction of interactive surface fluxes — these should only be specified for the last two hours, so as to avoid excess fluxes from winds which are initially too large.

Before integrating any case, we ask all investigators to double check that their initial cloud base is within 10m of 600m, and that cloud top liquid water contents are near 0.45 gkg^{-1} .

In addition we ask investigators to volunteer sensitivity studies, these would be most helpful if they explored resolution issues, as well as physical issues such as the role of surface fluxes, or moisture jumps across the inversion. Because we realize that the computations can be rather intensive and beyond the capacity of some groups we ask that all groups perform at least the first computation, and preferably the first three itemized above.

5. Desired Output

For all simulations we ask for the following sets of statistics:

Set T: Timeseries

1. Time since start of simulation [s].
2. Average height z_i [m], associated with $\theta_l = 295 \text{ K}$ contour.
3. $\overline{z_i'^2}$ [m^2].
4. Average height, z_b , of cloud base (over columns with cloud).
5. $\overline{z_b'^2}$ (over columns with cloud). [m^2].
6. Fraction of columns with cloud (in percent) [%].
7. Domain averaged liquid water path [gm^{-2}].
8. Liquid water path variance [g^2m^{-4}].

9. Vertically integrated TKE (resolved and subfilter) averaged over domain [kg/s^2] (note implied density multiplication).
10. $\overline{w'^2}|_{max}$ Maximum value of $\overline{w'^2}$ in domain [ms^{-1}].
11. w_* , defined as the vertically integrated buoyancy flux [ms^{-1}].
12. Average surface latent heat flux [Wm^{-2}].
13. Average surface sensible heat flux [Wm^{-2}].
14. Average value of u_* [ms^{-1}].

Set A: Mean State

1. Height at which variables in this set locate [m].
2. \bar{u} [ms^{-1}].
3. \bar{v} [ms^{-1}].
4. $\bar{\theta}_l$ [K].
5. \bar{r}_t Water (gas+liquid phases) mixing ratio [gkg^{-1}]
6. \bar{r}_l Water (liquid phase) mixing ratio [gkg^{-1}]
7. ρ_0 Reference density [kg/m^3]

Set B: Variances & Skewness

1. Height at which variables in this set locate [m].
2. Resolved $\overline{u'^2}$ [$\text{m}^2 \text{s}^{-2}$].
3. Resolved $\overline{v'^2}$ [$\text{m}^2 \text{s}^{-2}$].
4. Resolved $\overline{w'^2}$ [$\text{m}^2 \text{s}^{-2}$].
5. Resolved $\overline{w'^3}$ [$\text{m}^3 \text{s}^{-3}$].
6. Resolved $\overline{r_l'^2}$ [$\text{g}^2 \text{kg}^{-2}$].
7. Resolved $\overline{r_t'^2}$ [$\text{g}^2 \text{kg}^{-2}$].
8. Resolved $\overline{\theta_l'^2}$ [K^2].

Set C: Fluxes

1. Height at which variables in this set locate [m].
2. Radiative flux [Wm^{-2}].
3. Total θ_l flux [Wm^{-2}].
4. SGS θ_l flux [Wm^{-2}].
5. Total r_t flux [Wm^{-2}].
6. SGS r_t flux [Wm^{-2}].
7. Total u flux [m^2s^{-2}].
8. SGS u flux [m^2s^{-2}].
9. Total v flux [m^2s^{-2}].
10. SGS v flux [m^2s^{-2}].

Set D: TKE-Budget

1. Height at which variables in this set locate [m].
2. E (Resolved TKE) [$\text{m}^2 \text{s}^{-2}$].
3. Resolved shear production [$\text{m}^2 \text{s}^{-3}$].
4. Resolved buoyancy production [$\text{m}^2 \text{s}^{-3}$].
5. Resolved transport (turbulent plus pressure) [$\text{m}^2 \text{s}^{-3}$].
6. Dissipation [$\text{m}^2 \text{s}^{-3}$].
7. Storage ($\frac{E(t_1)-E(t_2)}{t_1-t_2}$) [$\text{m}^2 \text{s}^{-3}$].
8. SGS buoyancy production [$\text{m}^2 \text{s}^{-3}$].
9. e (SGS TKE) [$\text{m}^2 \text{s}^{-2}$].

Set T is desired for at an interval of 300s or less for the entire duration of the simulation. Sets A is required for the first time step, and Sets A-D are to be provided for 30 minute averaging intervals for the duration of the simulation.

6. Wait, Stop, Check!

Things worth checking before you run:

- Winds: are the winds set correctly? In previous versions of the document we had set U_g and V_g to 6 and -4.25 ms^{-1} respectively, in accord with the observed mixed layer. However, we are now asking that they be set to larger magnitudes 7 and -5.5 ms^{-1} respectively, so that the mixed layer values come into approximate balance with the observations.
- Cloud: are the initial cloud characteristics (base at 600m, cloud top liquid water near 0.45 gkg^{-1} correct?
- Are you using the prescribed surface fluxes correctly? Is subsidence turned off for initial runs?

References

- Bretherton, C. S., M. MacVean, P. Bechtold, A. Chlond, W. Cotton, J. Cuxart, H. Cuijpers, M. Khairoutdinov, B. Kosovic, D. Lewellen, C.-H. Moeng, P. Siebesma, B. Stevens, D. Stevens, I. Sykes and M. Wyant, 1999: An intercomparison of radiatively-driven entrainment and turbulence in a smoke cloud, as simulated by different numerical models. *Quart. J. Roy. Meteor. Soc.*, **125**, 391–423.
- Fu, Q. and K.-N. Liou, 1993: Parameterization of the radiative properties of cirrus clouds. *J. Atmos. Sci.*, **50**, 2008–2025.
- Moeng, C.-H. and R. Rotunno, 1990: Vertical-velocity skewness in the buoyancy-driven boundary layer. *J. Atmos. Sci.*, **47**, 1149–1162.
- Moyer, K. A. and G. S. Young, 1991: Observations of vertical velocity skewness within the marine stratocumulus-topped boundary layer. *J. Atmos. Sci.*, **48**, 403–410.
- Siems, S. T., D. H. Lenschow and C. S. Bretherton, 1993: A numerical study of the interaction between stratocumulus and the air overlying it. *J. Atmos. Sci.*, **50**, 3663–3676.
- Stevens, B., 2002: Entrainment in stratocumulus mixed layers. *Quart. J. Roy. Meteor. Soc.*, **128**, 2663–2690.
- Stevens, B., D. H. Lenschow, C.-H. M. Ian Faloona, D. K. Lilly, B. Blomquist, G. Vali, A. Bandy, T. Campos, H. Gerber, S. Haimov, B. Morley and D. Thorton, 2003: On entrainment in nocturnal marine stratocumulus. *Quart. J. Roy. Meteor. Soc.*, **129**, accepted.